Oxidatively Modified Calmodulin Binds to the Plasma Membrane Ca-ATPase in a Nonproductive and Conformationally Disordered Complex

Jun Gao, Yihong Yao, and Thomas C. Squier
Biochemistry and Biophysics Section, Department of Molecular Biosciences, University of Kansas, Lawrence, Kansas 66045 USA

ABSTRACT Oxidation of either Met^{145} or Met^{146} in wheat germ calmodulin (CaM) to methionine sulfoxide prevents the CaM-dependent activation of the plasma membrane (PM) Ca-ATPase (D. Yin, K. Kuczera, and T. C. Squier, 2000, *Chem. Res. Toxicol*. 13:103–110). To investigate the structural basis for the inhibition of the PM-Ca-ATPase by oxidized CaM (CaM_{ox}), we have used circular dichroism (CD) and fluorescence spectroscopy to resolve conformational differences within the complex between CaM and the PM-Ca-ATPase. The similar excited-state lifetime and solvent accessibility of the fluorophore *N*-1-pyrenyl-maleimide covalently bound to Cys^{26} in unoxidized CaM and CaM_{ox} indicates that the globular domains within CaM_{ox} assume a native-like structure following association with the PM-Ca-ATPase. However, in comparison with oxidized CaM there are increases in the 1) molar ellipticity in the CD spectrum and 2) conformational heterogeneity between the opposing globular domains for CaM_{ox} bound to the CaM-binding sequence of the PM-Ca-ATPase. Furthermore, CaM_{ox} binds to the PM-Ca-ATPase with high affinity at a distinct, but overlapping, site to that normally occupied by unoxidized CaM. These results suggest that alterations in binding interactions between CaM_{ox} and the PM-Ca-ATPase block important structural transitions within the CaM-binding sequence of the PM-Ca-ATPase that are normally associated with enzyme activation.

INTRODUCTION

Calcium has evolved as the major signaling molecule in all eukaryotes, and functions to modulate intracellular metabolism to rapidly coordinate a range of diverse cellular processes involved in neurotransmission, neuronal plasticity, muscle contraction, and a host of reactions involved in the energy and biosynthetic metabolism of the cell (Williams, 1999; Chin and Means, 2000). Critical to these calcium signaling mechanisms is the maintenance of the large (i.e., 10,000-fold) concentration gradient by the plasma membrane (PM) Ca-ATPase, which permits rapid and localized increases in cytosolic calcium upon modulation of calcium channel function. The maintenance of these steep calcium gradients represents a major energy expenditure within excitable cells and through respiratory control mechanisms is tightly coupled to rates of oxidative phosphorylation and the generation of reactive oxygen species (ROS). Therefore, observed decreases in rates of calcium release and re-sequestration under a range of pathological conditions, including biological aging, have the potential to reduce both energy consumption and the concomitant production of ROS. Thus, observed changes in calcium homeostasis following oxidative stress may represent adaptive responses that enhance the probability of cellular survival (Katz, 1992; Gao et al., 1998b). However, a quantitative understanding of how environmental stresses regulate calcium homeostasis requires an understanding of the structural consequences of post-translational modifications within key calcium regulatory proteins. In this respect, specific sites of oxidative modification have been identified in calmodulin (CaM) and the Ca-ATPase expressed in sarcoplasmic reticulum membranes that occur in response to oxidative stress (Gao et al., 1998b; Viner et al., 1999). During normal biological aging methionines in CaM are oxidized to their corresponding methionine sulfoxides, whereas the specific nitration of tyrosines in the Ca-ATPase results in an age-related loss of function. Of these two types of post-translational modifications, the oxidation of methionines is reversible and has been suggested to play a regulatory role in coupling calcium signaling to cellular redox conditions through the modulation of CaM function (Vogt, 1995; Sun et al., 1999; Yermolaieva et al., 2000; Squier and Bigelow, 2000).

A determination of the possible regulatory role of methionine oxidation in modulating CaM function requires that a causative linkage be identified between the oxidation of specific methionines and alterations in CaM function or structure. In this regard, it has been demonstrated that the oxidation of a methionine near the carboxy terminus to form the corresponding methionine sulfoxide results in an inability to activate the PM-Ca-ATPase (Yao et al., 1996b; Yin et al., 2000). In contrast, oxidation of the other seven methionines in CaM does not affect the ability to fully activate the PM-Ca-ATPase in the presence of saturating concentrations of CaM (Yin et al., 2000a). Furthermore, CaM can fully activate the PM-Ca-ATPase following the replacement of the majority of the methionines in either domain with polar glutamine (Yin et al., 1999). Therefore, the binding energy associated with methionine side-chain interactions and sequences within the CaM-binding sequence of the PM-Ca-ATPase are not critical to enzyme activation. These results suggest that oxidant-induced global conformational changes may prevent enzyme activation because of alterations in the

Received for publication 11 August 2000 and in final form 15 January 2001.

Address reprint requests to Dr. Thomas C. Squier, University of Kansas, Biochemistry. and Biophysics Section, Department of Molecular Biosciences, 5055 Haworth Hall, Lawrence, KS 66045-2106. Tel.: 785-864-4008; Fax: 785-864-5321; E-mail: tsquier@ukans.edu.

0006-3495/01/04/1791/11 $2.00

binding mechanism, which normally involves the ordered and cooperative association of both domains with the CaM-binding sequence of the PM-Ca-ATPase (Gao et al., 1998a; Sun et al., 2000).

To address the underlying mechanisms associated with the inability of CaM_{ox} to activate the PM-Ca-ATPase, we have used circular dichroism (CD) and fluorescence spectroscopy to measure the dynamic structure of CaM_{ox} bound to the CaM-binding sequence of the PM-Ca-ATPase. Wheat germ CaM, which possesses 91% sequence identity to vertebrate CaM, was chosen for these measurements due to sequence differences near the carboxy terminus that result in the preferential oxidation of Met^{145} or Met^{146} (Yao et al., 1996b; Yin et al., 2000). CaM_{ox} was generated using H_2O_2 to selectively oxidize an average of 1.5 ± 0.1 methionines per CaM to methionine sulfoxide. Under these conditions either Met^{145} or Met^{146} is oxidized in 60 ± 10% of all CaM molecules (Yao et al., 1996b). The oxidation of these methionines has previously been shown to result in 1) global structural changes involving the backbone fold of apo- and calcium-activated CaM and 2) an inability to activate the PM-Ca-ATPase (Yao et al., 1996b; Gao et al., 1998a; Yin et al., 2000). Although methionines other than Met^{145} and Met^{146} are also oxidized to a small extent in these samples, their oxidation does not affect either the function or backbone fold of CaM (Gao et al., 1998a; Yin et al., 1999, 2000). This latter result agrees with earlier observations that the oxidative modification of most methionines does not affect protein structure or function (Levine et al., 1996, 1999; Berlett and Stadtman, 1997). Therefore, CaM containing oxidatively modified methionines at positions other than Met^{145} or Met^{146} has a native-like structure, permitting an analysis of the functional and structural effects resulting from the oxidative modification of Met^{145} or Met^{146} (Gao et al., 1998a).

Measurements of the structure of CaM bound to the PM-Ca-ATPase are facilitated by the presence of a single cysteine (Cys^{26}) and a single tyrosine (Tyr^{138}) in the opposing globular domains of wheat germ CaM, which provide the opportunity for selective chemical modification. *N*-1(-pyrenyl) maleimide (PMal) was used to label Cys^{26} and provided a fluorescence signal that allowed the measurement of the binding and conformation of CaM_{ox} to the CaM-binding sequence within the PM-Ca-ATPase. Tyr^{138} was selectively nitrated with tetranitromethane (TNM), which acts to red-shift the absorbance properties of the resulting nitrotyrosine, permitting its use as a fluorescence resonance energy transfer (FRET) acceptor to measure the spatial separation and conformational heterogeneity between the opposing domains of CaM (Steiner et al., 1991; Yao et al., 1994). We find that the globular domains in CaM_{ox} assume a native-like structure upon association with the PM-Ca-ATPase. However, in comparison with unoxidized CaM, there is 1) an increase in the molar ellipticity in the CD spectrum and 2) increased conformational heterogeneity between the opposing globular domains of CaM_{ox} bound to the CaM-binding sequence of the PM-Ca-ATPase. These results suggest that CaM_{ox} binding to the PM-Ca-ATPase fails to induce the normal secondary structural changes within the CaM-binding sequence that are essential for enzyme activation.

MATERIALS AND METHODS

Materials

Hydrogen peroxide (H_2O_2) was obtained from Fisher (Pittsburgh, PA). PMal was supplied from Molecular Probes (Junction City, OR). TNM was purchased from Aldrich (Milwaukee, WI). C25W (QILWFRGLNRIQTQIRVVNAFRSSC) and C28W (LRRGQILWFRGLNRIQTQIRVVNAFRSS) peptides were, respectively, synthesized and HPLC purified by the Kansas State University Biotechnology Microchemical Core Facility (Manhattan, KS) and Commonwealth Biotechnologies (Richmond, VA). Wheat germ CaM was purified as previously described (Strasburg et al., 1988). Porcine erythrocyte ghost membranes were prepared essentially as described by Penniston and co-workers (Niggli et al., 1979; Yao et al., 1996a). Purified wheat germ CaM and erythrocyte ghost membranes were stored at −70°C.

Specific derivitization of CaM

The chemical modification of Cys^{26} with PMal and Tyr^{138} with TNM was carried out as previously described (Yao et al., 1994). The concentration of CaM was determined using the micro BCA assay obtained from Pierce (Rockford, IL), using a stock solution of desalted bovine CaM whose concentration was determined using the published extinction coefficient for bovine CaM, where $\epsilon_{277} = 3029\ M^{-1}\ cm^{-1}$ (Strasburg et al., 1988).

Oxidative modification of methionines in CaM

The selective oxidative modification of methionines in wheat germ CaM to the corresponding methionine sulfoxides involved the exposure of 60 μM wheat germ CaM (1.0 mg/ml) in 50 mM HOMOPIPES (pH 5.0), 1 mM $MgCl_2$, 0.1 mM $CaCl_2$, and 0.1 M KCl to 5 mM H_2O_2 for 10 h at 25°C. Under these conditions, an average of 1.5 ± 0.1 methionines are oxidatively modified in each CaM, ~60 ± 10% of all CaM species contain an oxidatively modified methionine near the carboxy terminus (either Met^{145} or Met^{146}), and there is a 60% reduction in the maximal CaM-dependent activation of the PM-Ca-ATPase (Yao et al., 1996b; Gao et al., 1998a; Yin et al., 2000). The concentration of H_2O_2 was determined using the molar extinction coefficient $\epsilon_{240} = 39.4 \pm 0.2\ M^{-1}\ cm^{-1}$ (Nelson and Kiesow, 1972).

CaM binding to the PM-Ca-ATPase in erythrocyte ghost membranes

CaM binding to the PM-Ca-ATPase involved the incubation of variable amounts of CaM with 6.0 mg of porcine erythrocyte ghost membranes in a total volume of 1 ml in a buffer composed of 0.1M HEPES (pH 7.5), 0.1 M KCl, 1 mM $MgCl_2$, and 0.1 mM $CaCl_2$ (buffer A), essentially as previously described (Yao et al., 1996a). Following incubation on ice for 15 min in the dark, the sample was centrifuged at 31,000 × g_{max} for 20 min. The pellet was resuspended in the same buffer and centrifuged to remove unbound CaM_{ox} from the erythrocyte ghost membranes before being resuspended in buffer A at a final protein concentration of 6 mg/ml. Measurements of the binding stoichiometry of CaM to the PM-Ca-ATPase used PMal-labeled unoxidized CaM and CaM_{ox}, whose fluorescence sig-

nals provide a sensitive means to detect the amount of bound CaM. The amount of bound CaM was measured following its dissociation from erythrocyte ghost membranes (upon addition of 0.1 mM EGTA) in conjunction with a standard curve obtained using known concentrations of either PMal-CaM or PMal-CaM_{ox}. The Ca-ATPase activity of the erythrocyte ghosts was determined from the initial rate of phosphate release following the addition of 5 mM ATP in buffer A (Lanzetta et al., 1979). The erythrocyte ghost membrane protein concentration was determined by the Biuret method (Gornal et al., 1949).

Circular dichroism spectroscopy

CD spectra were measured using a Jasco J-710 spectropolarimeter (Jasco Corp., Tokyo, Japan) and a temperature-jacketed spectral cell with a pathlength of 0.1 cm. The concentration of the peptide (i.e., C25W or C28W) corresponding to the CaM-binding sequence of the PM-Ca-ATPase was determined using the published extinction coefficient, where ϵ_{280} = 5600 M^{-1} cm^{-1} (Chapman et al., 1992). Desalted CaM (50 μg/ml) was dissolved in 10 mM Tris-HCl (pH 7.5), 0.1 M $KClO_4$, 1 mM $Mg(ClO_4)_2$, and 0.1 mM $Ca(ClO_4)_2$, and spectra were recorded at 1-nm intervals between 190 and 265 nm.

Fluorescence measurements

Excitation of PMal-CaM involved the 351-nm line from an Innova 400 argon ion laser (Coherent, Santa Clara, CA), and fluorescence was detected with an ISS K2 frequency domain fluorometer, as described previously (Yao et al., 1994, 1996a). Emission slits were adjusted to a 4-nm bandwidth, and the sample temperature was maintained at 25°C. In the case of PMal-CaM_{ox} bound to the peptide C25W, the fluorescence emission was detected subsequent to a Schott GG400 long-pass filter. In the case of PMal-CaM_{ox} bound to the PM-Ca-ATPase in erythrocyte ghosts (0.25 mg/ml), emitted light was detected following a combination of a Schott GG400 long-pass filter and an Oriel band-pass filter centered at 420 nm (full-width at half-maximum is 10 nm). Steady-state fluorescence quenching involved the addition of the spin label TEMPAMINE in microliter increments to a 2.0-ml sample in buffer A containing either 1) 1.2 μM PMal-CaM_{ox} and 3.6 μM C25W or 2) 10 μM PMal-CaM_{ox} bound to the PM-Ca-ATPase (i.e., 0.25 mg/ml erythrocyte ghost membranes whose high-affinity CaM-binding sites are saturated with PMal-CaM_{ox}).

Frequency-domain fluorescence data analysis

Explicit expressions, previously described in detail, permit the ready calculation of the lifetime components (i.e., α_i and τ_i) relating to a multiexponential decay (Weber, 1981; Lakowicz et al., 1985) or the Gaussian distribution of distances between donor and acceptor chromophores (Haas et al., 1978; Beechem and Haas, 1989; Cheung, 1991), where

$$\Phi_{c\omega} = \arctan\frac{N_\omega}{D_\omega} \text{ and } m_{c\omega} = \sqrt{N_\omega^2 + D_\omega^2}. \quad (1)$$

Alternatively, algorithms are available that permit the determination of the initial anisotropy in the absence of rotational diffusion (r_o), the rotational correlation times (ϕ_i), and the amplitudes of the total anisotropy loss associated with each rotational correlation time ($r_0 g_i$), as previously described in detail (Yao et al., 1994; Lakowicz et al., 1985, 1991a; Johnson and Faunt, 1992). In all cases, the transforms (i.e., N_ω and D_ω) can be readily modified to take into account a heterogeneous solution of CaM that contains two major structural conformers (i.e., unoxidized CaM and CaM_{ox}), where

$$N_{\omega_i} = f_{\text{oxidized}_i} \times N_{\text{oxidized}} + (1 - f_{\text{oxidized}_i}) \times N_{\text{native}} \quad (2)$$

and

$$D_{\omega_i} = f_{\text{oxidized}_i} \times D_{\text{oxidized}} + (1 - f_{\text{oxidized}_i}) \times D_{\text{native}}. \quad (3)$$

An independent measurement of the individual lifetime components or correlation times and associated amplitudes relating to unoxidized CaM (i.e., α_i and τ_i, or $g_i r_o$ and ϕ_i) permits the recovery of the lifetime or rotational correlation times associated with CaM_{ox} (Gao et al., 1998a). The parameter values are determined using the method of nonlinear least-squares analysis in which the reduced χ^2 (i.e., χ_R^2) is minimized (Bevington, 1969). A comparison of χ_R^2 values provides a quantitative assessment of the adequacy of different assumed models to describe the data (Lakowicz and Gryczynski, 1991a). Data were fit using the Globals software package (University of Illinois, Urbana-Champaign, IL) or the program Mathcad (MathSoft, Cambridge, MA).

RESULTS

CaM_{ox} binding to the PM-Ca-ATPase

The PM-Ca-ATPase contains a single binding sequence for CaM and is the only high-affinity CaM-binding protein in erythrocyte ghost membranes (Jarrett and Kyte, 1979; Hinds and Andreasen, 1981; Yao et al., 1996a). Therefore, to investigate how CaM_{ox} inhibits the PM-Ca-ATPase we have compared the relative affinities and stoichiometries of CaM_{ox} binding to the PM-Ca-ATPase in erythrocyte ghost membranes with unoxidized CaM. The use of erythrocyte ghost membranes to assess CaM-binding to the PM-Ca-ATPase, furthermore, avoids potential artifacts involving concentration-dependent alterations in the CaM-binding stoichiometry that occur following purification of the PM-Ca-ATPase (Kosk-Kosicka and Bzdega, 1988; Vorherr et al., 1991; Sackett and Kosk-Kosicka, 1996). The concentration dependence of binding is similar for unoxidized CaM and CaM_{ox}, with apparent saturation of all high-affinity binding sites occurring above 40 nM CaM (Fig. 1). Increasing the CaM concentration 50-fold results in no additional binding (data not shown), indicating that under these conditions all high-affinity CaM-binding sites are occu-

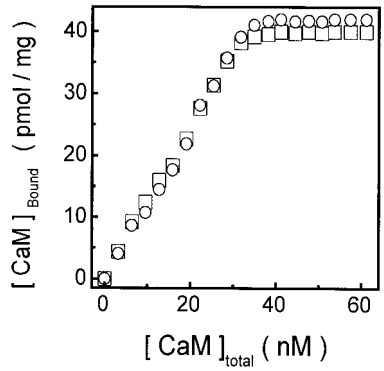

FIGURE 1 Binding of unoxidized CaM and CaM_{ox} to erythrocyte ghost membranes. Stoichiometries of unoxidized PMal-CaM (□) and PMal-CaM_{ox} (○) bound to porcine erythrocyte ghost membranes were measured after incubation for 15 min at 25°C in buffer A.

pied. Thus, the maximal binding stoichiometry of CaM to the PM-Ca-ATPase is not affected by oxidative modification.

To assess the relationship between the binding sites for unoxidized CaM and CaM_{ox} on the PM-Ca-ATPase, we have investigated the ability of CaM_{ox} to displace unoxidized CaM (labeled with the fluorophore PMal) bound to the PM-Ca-ATPase. A 20 ± 7% decrease in the amount of PMal-CaM bound to the PM-Ca-ATPase was observed upon incubation of PMal-CaM-saturated erythrocyte ghost membranes with a 10-fold molar excess of CaM_{ox} with no significant change in ATPase activity (Fig. 2, *A* and *C*). In contrast, a similar concentration of unoxidized CaM displaces 84 ± 6% of PMal-CaM bound to the PM-Ca-ATPase. In a complementary experiment, unoxidized CaM was found to displace 18 ± 4% of PMal-CaM_{ox} bound to the PM-Ca-ATPase (Fig. 2 *B*), with no significant change in the relative Ca-ATPase activity (Fig. 2 *D*). Addition of a 10-fold molar excess of CaM_{ox} to these erythrocyte ghost membranes resulted in an 80 ± 6% decrease in the amount of PMal-CaM_{ox} bound to the PM-Ca-ATPase (Fig. 2 *B*). These results suggest that CaM_{ox} can neither displace unoxidized CaM from its binding site on the PM-Ca-ATPase nor bind to additional binding sequences, and imply that there are overlapping binding sites on two conformationally different states of the PM-Ca-ATPase for CaM and CaM_{ox}. The small decrease in the amount of PMal-CaM bound to erythrocyte ghost membranes upon addition of CaM_{ox} (Fig. 2 *A*) is related to heterogeneity within the sample of oxidatively modified CaM, because 40 ± 10% of the total CaM is not oxidized at either Met^{145} or Met^{146} (Gao et al., 1998a). The decreased maximal ATPase activity associated with activation of the PM-Ca-ATPase by CaM_{ox} is in agreement with previous results, which demonstrated that the oxidation of Met^{145} or Met^{146} in wheat germ CaM prevents the CaM-dependent activation of the PM-Ca-ATPase (Yao et al., 1996b; Yin et al., 2000).

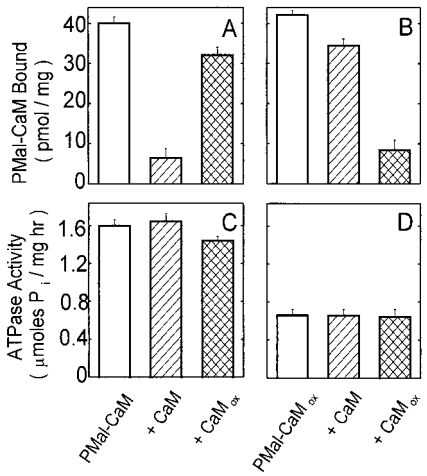

FIGURE 2 Competition between unoxidized CaM and CaM_{ox} for binding sites on the PM-Ca-ATPase. Amount of either unoxidized PMal-CaM (*A*) or PMal-CaM_{ox} (*B*) bound to the PM-Ca-ATPase and respective CaM-dependent enzymatic activity (*C* and *D*) before (*open bars*) and after the addition of 0.1 μM of either unoxidized CaM (*diagonal bars*) or CaM_{ox} (*hatched bars*) to erythrocyte ghost membranes. Experimental conditions involved 0.25 mg ml^{-1} erythrocyte ghost membranes in buffer A at 25°C.

Circular dichroism measurements of secondary structural changes

We have used CD spectroscopy to compare the secondary structures of unoxidized CaM and CaM_{ox} following calcium activation and binding to a peptide (C28W) corresponding to the CaM-binding sequence of the PM-Ca-ATPase. CaM has previously been shown to bind to this peptide with an affinity and tertiary structure that is virtually identical to that of the PM-Ca-ATPase ($K_d < 1$ nM) (Vorherr et al., 1990; Yao and Squier, 1996). Before peptide binding, the CD spectra of unoxidized CaM and CaM_{ox} are similar, suggesting that oxidation does not result in large changes in secondary structure (Fig. 3 *A*). In contrast, there are statistically significant differences in the intensity of the CD spectra as well as the ratio of the molar ellipticities centered near 208 nm ($\pi\pi^*$ parallel transition) and 222 nm ($n\pi^*$ parallel transition) (i.e., $[\theta]_{208}/[\theta]_{222}$) for unoxidized CaM and CaM_{ox} bound to C28W (Fig. 3 *B*). This result is in contrast to an array of different CaM mutants where peptide binding has been shown to restore a native-like CD spec-

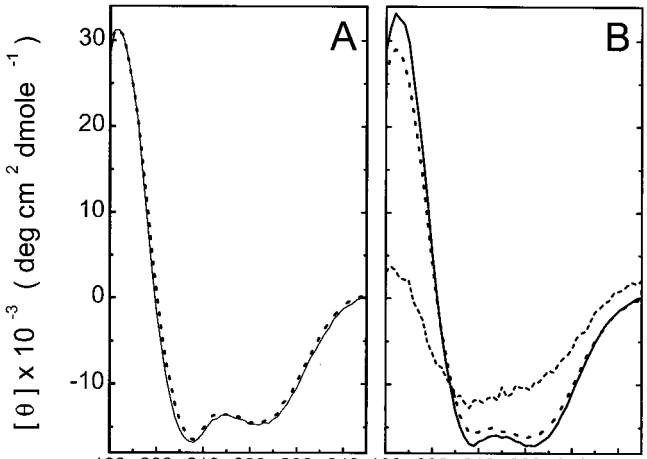

FIGURE 3 Circular dichroism spectra of unoxidized CaM and oxidatively modified CaM. CD spectra were acquired for unoxidized CaM (——) and CaM_{ox} (- - -) under conditions of calcium saturation (*A*) or after the binding to C28W (*B*). The spectrum of C28W is shown in *B* (· · ·). In all cases, the concentration of CaM was 3.6 μM, and when applicable, the concentration of C28W was 6.0 μM. The contribution of unbound C28W to the CD spectrum for the complex between CaM and C28W was subtracted. The experimental buffer contained 10 mM Tris-HCl (pH 7.5), 0.1 M $KClO_4$, 1 mM $Mg(ClO_4)_2$, and 0.1 mM $Ca(ClO_4)_2$. Temperature was 25°C.

trum (Haiech et al., 1991; Findlay et al., 1995; Browne et al., 1997), and suggests that the inability of CaM_{ox} to activate the PM-Ca-ATPase results from an aberrant conformation within the complex between CaM_{ox} and the CaM-binding sequence of the PM-Ca-ATPase.

Fluorescence measurements of the backbone fold of CaM

To detect potential structural differences between unoxidized CaM and CaM_{ox}, we have used fluorescence spectroscopy to measure the excited-state fluorescence lifetime and solvent accessibility of PMal covalently bound to Cys^{26} in CaM bound to the CaM-binding sequence of the PM-Ca-ATPase. These parameters have previously been shown to provide a sensitive measure of alterations in the backbone fold of CaM (Yao and Squier, 1996; Yao et al., 1996a,b; Gao et al., 1998b). For example, oxidation of Met^{145} or Met^{146} results in an approximately twofold decrease in the mean fluorescence lifetime ($\bar{\tau}$) and a corresponding twofold increase in the bimolecular quenching constant (k_q) for PMal-CaM (Gao et al., 1998a). Similar large changes in $\bar{\tau}$ and k_q are observed for PMal-CaM bound to either the PM-Ca-ATPase or peptides corresponding to different CaM-binding sequences (Yao and Squier, 1996; Yao et al., 1996a). In contrast to these earlier results, $\bar{\tau}$ is similar for unoxidized CaM and CaM_{ox} bound to the PM-Ca-ATPase (or C25W) (Table 1). Likewise, the solvent accessibilities of unoxidized PMal-CaM and PMal-CaM_{ox} bound to either C25W or the PM-Ca-ATPase to the water-soluble quencher TEMPAMINE are virtually identical to one another (Fig. 4), further suggesting that methionine oxidation does not result in large changes in the global fold of CaM. It should be noted that substantial differences in the fluorescence lifetime and solvent accessibilities of PMal-CaM bound to the PM-Ca-ATPase in erythrocyte ghosts or C25W arise because of additional steric and electrostatic interactions between CaM and structural elements outside the CaM-binding sequence of the PM-Ca-ATPase (Yao and Squier, 1996).

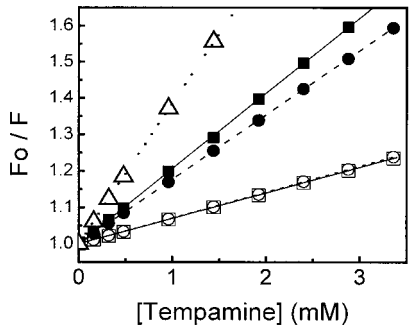

FIGURE 4 Solvent accesibilities of PMal covalently bound to Cys^{26} in unoxidized CaM and CaM_{ox}. Stern-Volmer plots are shown for unoxidized CaM (■ and □) and CaM_{ox} (● and ○) bound to the CaM-binding sequence of the PM-Ca-ATPase using either the isolated peptide (i.e., C25W) (■ and ●) or erythrocyte ghost membranes (□ and ○) relative to the unbound chromophore covalently modified with cysteine (i.e., PMal-Cys) (△). Experimental conditions involved 1.2 μM CaM in the presence of 3.6 μM C25W or 10 nM CaM bound to the PM-Ca-ATPase in erythrocyte ghost membranes (0.25 mg ml^{-1}) in buffer A at 25°C.

Spatial separation between opposing globular domains of CaM

CaM binding is known to stabilize the secondary structure of CaM-binding sequences within a range of different en-

TABLE 1 Lifetime data associated with PMal-CaM_{ox} binding to the PM-Ca-ATPase

Ligand	Sample	α_1	τ_1 (ns)	α_2	τ_2 (ns)	α_3	τ_3 (ns)	$\bar{\tau}$* (ns)	$\chi_R^{2\dagger}$
C25W peptide	CaM_{ox}								
	Donor	0.813 (0.002)	2.54 (0.08)	0.176 (0.002)	7.7 (0.2)	0.011 (0.002)	112 (14)	4.7 (0.4)	1.5 (54.8)
	Donor-acceptor	0.814 (0.002)	1.60 (0.09)	0.176 (0.003)	5.6 (0.2)	0.009 (0.003)	81 (2)	3.0 (0.4)	1.2 (12.7)
	Unoxidized CaM‡								
	Donor	0.78 (0.01)	2.14 (0.08)	0.200 (0.008)	9.8 (0.4)	0.016 (0.001)	104 (4)	5.3 (0.3)	0.7 (7.9)
	Donor-acceptor	0.78 (0.02)	1.54 (0.06)	0.200 (0.007)	7.3 (0.3)	0.016 (0.001)	76 (5)	3.9 (0.2)	1.3 (11.9)
Erythrocyte ghosts	CaM_{ox}								
	Donor	0.871 (0.004)	1.34 (0.09)	0.128 (0.008)	7.7 (0.4)	0.001 (0.001)	133 (60)	2.3 (0.3)	8.6 (33.2)
	Donor-acceptor	0.830 (0.006)	0.78 (0.08)	0.167 (0.003)	4.8 (0.1)	0.002 (0.001)	47 (14)	1.6 (0.1)	3.0 (17.4)
	Unoxidized CaM‡								
	Donor	0.86 (0.02)	0.85 (0.06)	0.130 (0.005)	5.8 (0.2)	0.005 (0.001)	52 (4)	1.7 (0.2)	2.2 (18.9)
	Donor-acceptor	0.87 (0.02)	0.74 (0.04)	0.125 (0.003)	5.0 (0.2)	0.005 (0.001)	43 (1)	1.5 (0.1)	0.8 (8.9)

Average amplitudes (α_i) and lifetimes (τ_i) were obtained from multi-exponential fits to frequency domain data collected for unoxidized CaM and CaM_{ox} covalently labeled at Cys^{26} with PMal in the absence (donor) and presence (donor-acceptor) of the FRET acceptor nitrotyrosine[138]. Experimental uncertainties are indicated within brackets and except for $\bar{\tau}$, where errors were propagated, represent the maximal variance associated with a rigorous analysis of the correlated errors between the five fitting parameters relative to the parameter of interest, as previously described (Bevington, 1969; Beechem et al., 1991).

*Mean fluorescence lifetime ($\bar{\tau} = \Sigma\alpha_i\tau_i$).

†The χ_R^2 for a two-exponential fit to the data is shown in parentheses for comparison purposes.

‡From Yao et al., 1996a. Experimental conditions involve either 1.2 μM CaM bound to 3.6 μM C25W or 10 nM CaM bound to 0.25 mg/ml of porcine erythrocyte ghost membranes in buffer A at 25°C.

zymes, including the PM-Ca-ATPase (Meador et al., 1992, 1993; Ikura et al., 1992; Elshorst et al., 1999). This structural transition is reflected in the large reduction in the conformational heterogeneity between the opposing globular domains of CaM following association with the PM-Ca-ATPase (Yao et al., 1996a; Yao and Squier, 1996). Because this structural transition may be important to the mechanism of enzyme activation, it is of interest to investigate whether methionine oxidation affects the dynamic structure of CaM bound to the PM-Ca-ATPase. To accomplish this goal, we have used FRET to measure the average separation and distribution of distances between the opposing globular domains of CaM_{ox}. In these measurements, PMal covalently bound to Cys^{26} serves as the energy transfer donor, whereas nitrotyrosine^{138} serves as an energy transfer acceptor (Yao et al., 1994, 1996a). The frequency response and associated excited-state lifetimes of unoxidized CaM and CaM_{ox} are essentially unchanged (Table 1). In the presence of nitrotyrosine^{138} the frequency responses of the phase shift and modulation for both unoxidized CaM and CaM_{ox} are shifted to higher frequencies (Fig. 5), indicating the presence of FRET. In comparison with unoxidized CaM, the larger shift in the frequency response of CaM_{ox} indicates more FRET and a smaller spatial separation between the opposing globular domains in CaM_{ox} bound to the CaM-binding sequence of the PM-Ca-ATPase (Table 2). These results indicate that the tertiary structure of the complex between CaM_{ox} is different from that of unoxidized CaM.

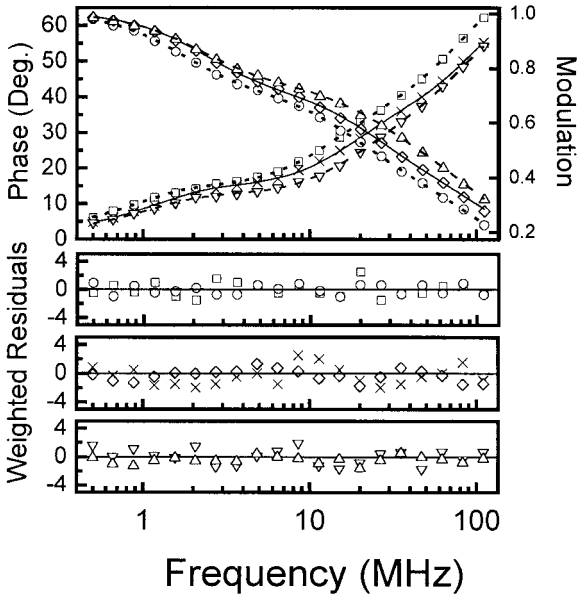

FIGURE 5 Fluorescence lifetime data of unoxidized CaM and CaM_{ox} bound to C25W. The frequency response of the phase shift (□, ×, and ▽) and modulation (○, ◇, and △) for unoxidized PMal-CaM (□, ×, ○, and ◇) and PMal-CaM_{ox} (▽ and △) in the absence (□ and ○) and presence (×, ◇, ▽, and △) of the FRET acceptor nitrotyrosine^{138}. Lines represent least-squares fits to a sum of exponentials (□ and ○) or to a Gaussian distribution of distances (×, ◇, ▽, and △). Weighted residuals correspond to the difference between the experimental data and the fit normalized by the experimental error associated with the phase (i.e., $\delta_{phase} = 0.2°$) and modulation (i.e., $\delta_{mod} = 0.005$). Measurements were made in buffer A at 25°C using 1.1 μM PMal-CaM and 3.3 μM C25W.

The spatial separation between the opposing globular domains of CaM_{ox} bound to the CaM-binding sequence of the PM-Ca-ATPase decreases by 2–3 Å in comparison with unoxidized CaM, irrespective of whether one assumes a unique conformation or a Gaussian distribution of distances (Table 2). The distance distribution between the opposing globular domains of CaM_{ox} bound to either C25W or the PM-Ca-ATPase are very similar (Table 2). These results suggest that the sequence within C25W contains the binding sequence for both unoxidized CaM and CaM_{ox}. However, in comparison with unoxidized CaM, there is a 5–9-Å increase in the half-width of the distance distribution for CaM_{ox} bound to either C25W or the PM-CA-ATPase (Table 2). The larger half-width of the Gaussian distance distribution for CaM_{ox} bound to the CaM-binding sequence of the PM-Ca-ATPase indicates that, in comparison with unoxidized CaM, there is greater conformational heterogeneity between the opposing globular domains of CaM_{ox} bound to the PM-Ca-ATPase. Because CaM_{ox} binds with a high affinity and the globular domains retain a native-like backbone fold, it is likely that the larger half-width of the distance distribution reflects increased conformational heterogeneity within the CaM-binding sequence. These results suggest that the CaM-binding sequence of the PM-Ca-ATPase is conformationally disordered following association with oxidized CaM. Alternatively, CaM_{ox} may bind to a distribution of sites within the CaM-binding sequence of the PM-Ca-ATPase. However, this latter possibility is unlikely because 1) the CaM-binding sequence for both unoxidized CaM and CaM_{ox} is contained within the 28-amino-acid peptide C28W and 2) the excited-state lifetimes and solvent accessibilities of PMal bound to Cys^{26} in unoxidized CaM and CaM_{ox} bound to the CaM-binding sequence of the PM-Ca-ATPase are virtually identical (see above).

Rotational dynamics of CaM

The rotational correlation times obtained for CaM bound to the CaM-binding sequences of the PM-Ca-ATPase are virtually identical to that of CaM bound to either CaM-dependent protein kinase IIα or smooth muscle myosin light chain kinase, whose crystal structures have been solved (Meador et al., 1992, 1993). These results suggest that the dynamic structure of CaM bound to the PM-Ca-ATPase is similar to that observed in the high-resolution structures available for CaM-dependent protein kinase IIα and smooth muscle myosin light chain kinase. The longest rotational correlation time accurately measures the hydrodynamic volumes of CaM bound to these target peptides ($\phi_{measured} = 10.6 \pm 0.4$ ns; $\phi_{calculated} \approx 10.6$ ns) (Yao and Squier, 1996) and pro-

TABLE 2 Donor-acceptor separation between chromophores between opposing globular domains of CaM_{ox}

Ligand	Sample	E%*	R_0 (Å)	r_{app} (Å)	R_{av}† (Å)	HW† (Å)	χ^2_R
C25W peptide	CaM_{ox}	38 (6)	17.3 (0.2)	18.8 (0.8)	16.5 (11.1–17.6)	17.7 (14.1–27.0)	0.8
	Unoxidized CaM‡	27 (2)	17.6 (0.2)	20.8 (0.6)	20.9 (20.6–21.2)	8.5 (7.4–9.8)	1.6
Erythrocyte ghosts	CaM_{ox}	32 (5)	15.4 (0.3)	17.4 (0.6)	17.2 (15.7–19.2)	13.8 (3.9–16.7)	4.0
	Unoxidized CaM‡	15 (2)	14.7 (0.2)	19.6 (0.7)	20.2 (19.8–20.6)	8.6 (6.6–10.8)	2.1

Distance measurements were obtained from FRET measurements between PMal located at Cys^{26} and nitrotyrosine^{138}.
*Observed energy-transfer efficiencies obtained from changes in $\bar{\tau}$ of PMal-CaM upon nitration of Tyr^{138} (Table 1), where

$$E = 1 - \frac{\bar{\tau}_{da} - \bar{\tau}_d \times (1 - f_a)}{\bar{\tau}_d \times f_a} = \frac{R_o^6}{R_o^6 + r_{app}^6}.$$

E is the corrected FRET efficiency, which takes into account the incomplete nitration of tyrosine (i.e., $f_a = 0.95 \pm 0.04$), $\bar{\tau}_d$ is the average lifetime of PMal-CaM, $\bar{\tau}_{da}$ is the average lifetime of PMal-CaM in the presence of nitrotyrosine^{138}, r_{app} is the apparent spatial separation between PMal and nitrotyrosine, and R_o is the Förster critical distance where $E = 0.50$ (Fairclough and Cantor, 1978; Lakowicz et al., 1991b).
†The average donor-acceptor separation (R_{av}) and associated half-width (HW) for a Gaussian distribution of distances between donor and acceptor chromophores (Haas et al., 1978; Beechem and Haas, 1989; Yao and Squier, 1996). Indicated errors (in parentheses) were either propagated or, in the case of R_{av} and HW, were obtained from the error surfaces associated with each experimental parameter (Bevington, 1969; Beechem et al., 1991).
‡Data taken from Yao et al., 1996a. Experimental conditions involve either 1.2 μM PMal-CaM bound to 3.6 μM C25W or 10 nM PMal-CaM bound to 0.25 mg/ml of porcine erythrocyte ghost membranes in buffer A at 25°C.

vides a sensitive measure of possible conformational changes within the complex between CaM_{ox} and the CaM-binding sequence of the PM-Ca-ATPase that arise because of methionine oxidation. It is, therefore, of interest to measure the rotational dynamics of the complex between CaM_{ox} and the CaM-binding sequence within the PM-Ca-ATPase (C25W).

The frequency response of the differential phase and modulated anisotropy of the complex between CaM_{ox} and C25W is shifted toward higher frequencies compared with the complex between unoxidized CaM and C25W, indicating the presence of faster rotational motion on the nanosecond time scale (Fig. 6). The data can be adequately described by a model involving two rotational correlation times, as indicated by the nearly randomly weighted residuals. Inclusion of additional rotational correlation times results in no significant improvement in χ^2_R (Table 3). The measured rotational correlation times of CaM_{ox} bound to C25W ($\phi_1 = 0.2 \pm 0.1$ ns; $\phi_2 = 18 \pm 4$ ns) are substantially different from those of unoxidized CaM ($\phi_1 = 0.9 \pm 0.1$ ns; $\phi_2 = 10.3 \pm 0.5$ ns), indicating large differences in their respective structures. The shorter rotational correlation time (ϕ_1) has previously been demonstrated to reflect the backbone fold of the bound peptide and the independent rotational dynamics of pyrene fluorophore, whereas the longer rotational correlation time (ϕ_2) is inversely related to the overall dimensions of the complex (Yao and Squier, 1996). In this respect, it is important to emphasize that the independent rotational dynamics of either domain of CaM is ~6–7 ns (Barbato et al., 1992), indicating that both domains of CaM remain structurally coupled through their association with the CaM-binding sequence of the PM-Ca-ATPase. Thus, in comparison with unoxidized CaM, there is a large increase in both the rotational dynamics of the backbone fold and in the overall dimensions of the complex between CaM_{ox} and C25W. These latter results suggest that the CaM-binding sequence remains conformationally disordered following association with CaM_{ox}.

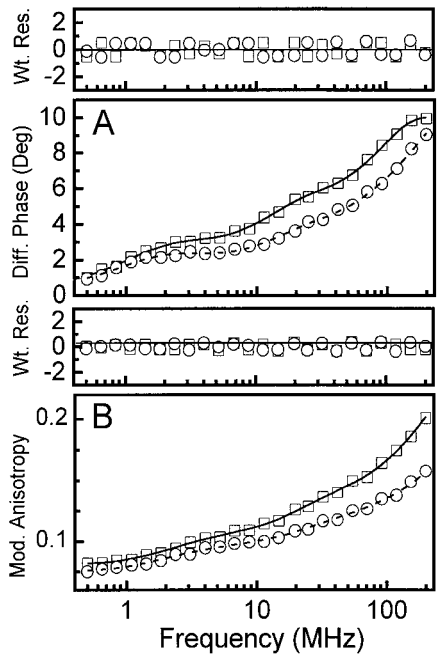

FIGURE 6 Rotational dynamics of unoxidized CaM and CaM_{ox} bound to C25W. Differential phase (*A*) and modulated anisotropy (*B*) data for CaM (□) and CaM_{ox} (○) bound to the CaM-binding sequence of the PM-Ca-ATPase and associated least-squares fits. Weighted residuals (Wt. Res.) are shown above each plot and represent the difference between the experimental and calculated values normalized by the errors for these respective measurements, which were 0.2° and 0.005 for the differential phase and modulated anisotropy. Experimental conditions involved 1.1 μM CaM in the presence of 3.3 μM C25W in buffer A at 25°C.

TABLE 3 Rotational dynamics of the complex between CaM and the CaM-binding sequence of the PM-Ca-ATPase

Sample	P*	g_1r_0	ϕ_1 (ns)	g_2r_0	ϕ_2 (ns)	$\chi_R^{2\dagger}$
CaM_{ox}	0.157 (0.004)	0.18 (0.01)	0.2 (0.1)	0.09 (0.01)	18 (4)	1.5 (22.5)
CaM‡	0.138 (0.002)	0.17 (0.01)	0.9 (0.1)	0.10 (0.01)	10.3 (0.5)	0.78 (10.4)

Average values for rotational correlation times (ϕ_i) and associated amplitude values (g_ir_0) were obtained from multi-exponential fits, where r_0 and g_i are, respectively, the initial anisotropy in the absence of rotational diffusion and the pre-exponential term. The reported uncertainties are obtained from error surfaces using the F-statistic and represent the maximal variance associated with one-standard deviation (Beechem et al., 1991).

*P is the steady-state polarization, where $P_{calculated} = f_{ox} \times P_{ox} + (1 - f_{ox}) \times P_{native}$ and $f_{ox} = 0.6$.

†The numbers in parentheses represents the χ_R^2 obtained from a one-component fit to the data.

‡Data taken from Yao and Squier, 1996. Experimental conditions involve either 1.2 μM PMal-CaM bound to 3.6 μM C25W or 10 nM PMal-CaM bound to 0.25 mg/ml of porcine erythrocyte ghost membranes in buffer A at 25°C.

DISCUSSION

Summary of results

Oxidatively modified CaM binds to the PM-Ca-ATPase but does not induce the formation of a stabilized secondary structure within the CaM-binding sequence that is normally associated with enzyme activation. Thus, in comparison with unoxidized CaM, the complex between CaM_{ox} and the CaM-binding sequence of the PM-Ca-ATPase displays 1) an increase in the molar ellipticity apparent in the CD spectrum (Fig. 3), 2) a smaller average spatial separation and a larger amount of conformational heterogeneity between the opposing globular domains (Table 2; Fig. 5), and 3) alterations in rotational mobility that suggest a larger degree of dynamic disorder associated with the structure of the CaM-binding peptide (Table 3; Fig. 6). The inability of oxidized CaM to induce the normal structural transitions associated with enzyme activation is not the result of the loss of specific binding interactions involving methionine side chains, because the nonconservative substitution of glutamine for methionine does not affect the ability of CaM to fully activate the PM-Ca-ATPase (Yin et al., 1999). Likewise, in agreement with earlier measurements in which large differences in the secondary and tertiary structures of mutant CaMs were largely abolished upon binding to target peptides (Findlay et al., 1995; Browne et al., 1997), the global fold of oxidized CaM assumes a native-like structure upon association with the CaM-binding sequence of the PM-Ca-ATPase (Figs. 4 and 5; Table 2). This latter result is consistent with the similar affinities and maximal binding stoichiometries of unoxidized CaM and CaM_{ox} for the PM-Ca-ATPase (Figs. 1 and 2). These results suggest that inhibition of the PM-Ca-ATPase by CaM_{ox} is the result of an altered binding mechanism that results in the formation of new and different contact interactions that fail to induce the normal secondary structural changes within the CaM-binding sequence associated with enzyme activation.

Relationship to other studies

The CaM-binding site on the PM-Ca-ATPase consists of ~25 amino acids that are highly basic and have a strong propensity to form amphipathic α-helices (James et al., 1988; Falchetto et al., 1991; Crivici and Ikura, 1995). Activation of the PM-Ca-ATPase by CaM involves the site-specific binding of the carboxyl-terminal domain of CaM followed by the structural collapse and association of the amino-terminal domain (Sun et al., 2000). CaM-binding sequences within a range of CaM-regulated enzymes have little discernable secondary structure before CaM binding, but generally assume an α-helical conformation 16–17 amino acids in length upon binding CaM (O'Neil and DeGrado, 1990; Meador et al., 1992, 1993; Trewhella, 1992; Ikura et al., 1992; Afshar et al., 1994). A similar structural transition occurs upon CaM binding to the PM-Ca-ATPase, as the dynamic structure of the complex between CaM and the CaM-binding sequence of the PM-Ca-ATPase is virtually identical to that of CaM bound to the CaM-binding sequences of CaMKIIα and MLCK (Meador et al., 1992, 1993; Trewhella, 1992; Ikura et al., 1992; Afshar et al., 1994; Yao and Squier, 1996; Yao et al., 1996a). Furthermore, the first 12 amino acids within a 20-amino-acid fragment derived from the CaM-binding sequence of the PM-Ca-ATPase forms an α-helical structure following association with the carboxyl-terminal domain of CaM (Elshorst et al., 1999). These results indicate that the specific binding of the carboxyl-terminal domain of unoxidized CaM to the CaM-binding sequence of the PM-Ca-ATPase induces the formation of an α-helical structure. Therefore, the inability of CaM_{ox} to induce the formation of an ordered secondary structure within the CaM-binding sequence probably results from an incorrect initial association involving the carboxyl-terminal domain, which does not induce the normal structural transition within the CaM-binding sequence associated with activation of the PM-Ca-ATPase. The observation that the CaM-binding sequence of the PM-Ca-ATPase before enzymatic activation by CaM is conformationally disordered is consistent with the disordered CaM-binding sequence in the crystal structure of CaM-dependent protein kinase I (Goldberg et al., 1996). Thus, the ability of CaM binding to induce an ordered protein secondary structural element may be a general feature involving the CaM-dependent activation of target proteins.

The inability of CaM_{ox} to activate the PM-Ca-ATPase is consistent with the observation that site-specific mutations in CaM can greatly decrease the extent of enzyme activation associated with CaM binding (Mukherjea et al., 1996; George et al., 1996; Meyer et al., 1996; Chin and Means, 1996; Chin et al., 1997a,b). For example, a CaM mutant involving the site-directed mutation of $Met^{144} \rightarrow Val^{144}$ fails to active nitric oxide synthase and functions as a competitive antagonist with respect to its activation by wild-type CaM (Kondo et al., 1999). This latter result is of particular significance, because valine and methionine sulfoxide both disrupt α-helical structures and would, therefore, be expected to perturb the structure of CaM (Richardson and Richardson, 1989; Dado and Gellman, 1993; Schenck et al., 1996). In contrast, mutations expected to preserve α-helical secondary structures (i.e., $Met^{144} \rightarrow Leu^{144}$ or $Met^{144} \rightarrow Phe^{144}$) retain the ability to fully activate nitric oxide synthase (Kondo et al., 1999). These latter results suggest that the disruption of the carboxyl-terminal α-helix results in the nonproductive binding of CaM to some target proteins, including the PM-Ca-ATPase.

The functional sensitivity of CaM to oxidation is unusual and arises because of the large abundance of surface-exposed and functionally important methionine residues (Yao et al., 1996b; Yin et al., 2000). In contrast, 85–90% of methionines in most proteins are buried and are not expected to be sensitive to oxidative stress or to play functional roles (Rose et al., 1985; Richardson and Richardson, 1989). Thus, based on chemical principles and known aspects of protein structure, CaM was predicted, and then demonstrated, to be sensitive to oxidant-induced loss of function (Yao et al., 1996b; Gao et al., 1998b; Yin et al., 2000). For these reasons, it is likely that CaM is preferentially oxidized under cellular conditions of oxidative stress, which result in the increased generation of ROS (Sohal and Weindruch, 1996; Berlett and Stadtman, 1997; Driver et al., 2000).

The ability of CaM_{ox} to inhibit CaM-dependent target enzymes, including calcium pumps, has the potential to result in the blunted and prolonged calcium transients characteristic of aging neurons (Verkhratsky et al., 1994; Yao et al., 1996b; Hühmer et al., 1996; Yin et al., 2000). Because the maintenance of intracellular calcium gradients is energetically expensive, and represents a major fraction of the total cellular ATP utilization, it is expected that the oxidation of CaM would result in decreased ATP utilization. In turn, decreases in cellular ATP consumption are expected to decrease flux through the electron transport chain in the mitochondria through respiratory control mechanisms. The decreased flux through the electron transport chain has the potential to reduce the associated generation of ROS, which have been estimated to represent ~2% of cellular oxygen consumption (Turrens, 1997). This may be important if impairments in the function of key components of oxidative metabolism, such as α-ketoglutarate dehydrogenase complex and aconitase, result in an increased production of ROS (Blass, 1996, 2000; Yan et al., 1997; Yan and Sohal, 1998; Gibson et al., 1999). Alternatively, down-regulation of flux through the electron transport chain resulting from decreases in energy metabolism or the oxidation of key transporters (e.g., the mitochondrial adenine nucleotide translocater) may compensate for a decreased functionality of electron transfer components (Yan and Sohal, 1998; Squier and Bigelow, 2000). By reducing the rate of ROS generation, normal cellular antioxidant defenses (e.g., superoxide dismutase and catalase), repair enzymes (e.g., MsrA), and degradative pathways (e.g., the proteasome) have the potential to selectively degrade or repair oxidized proteins (including CaM_{ox}) and restore cellular function (Sun et al., 1999; Ferrington et al., 2000; Squier and Bigelow, 2000).

Conclusions and future directions

We have demonstrated that oxidatively modified CaM binds at a conformationally distinct but overlapping site to that normally occupied by CaM and fails to stabilize the secondary structure within the CaM-binding sequence, which may be critical to enzyme activation. Additional measurements involving high-resolution structural methods using CaM mutants that permit site-specific oxidation are now needed to identify the detailed structural reasons underlying the inability of oxidatively modified CaM to activate the PM-Ca-ATPase. In addition, to clarify the cellular significance of CaM oxidation, it will be important to correlate the extent of CaM oxidation using intact cells to changes in calcium regulation, energy metabolism, and cellular survival following conditions of oxidative stress.

We thank Professors Diana J. Bigelow, Elias K. Michaelis, and Richard H. Himes for their insightful comments.

Supported by the National Institutes of Health (grants AG12993 and AG17996).

REFERENCES

Afshar, M., L. S. Caves, L. Guimard, R. E. Hubbard, B. Calas, G. Grassy, and J. Haiech. 1994. Investigating the high affinity and low sequence specificity of calmodulin binding to its targets. *J. Mol. Biol.* 244: 554–571.

Barbato, G., M. Ikura, L. E. Kay, R. W. Pastor, and A. Bax. 1992. Backbone dynamics of calmodulin studied by ^{15}N relaxation using inverse detected two-dimensional NMR spectroscopy: the central helix is flexible. *Biochemistry.* 31:5269–5278.

Beechem, J. M., E. Gratton, M. Ameloot, J. R. Knutson, and L. Brand. 1991. The global analysis of fluorescence intensity and anisotropy decay data: second generation theory and programs. *In* Topics in Fluorescence Spectroscopy, Vol. 2. J. R. Lakowicz, editor. Plenum Press, New York. 1–52.

Beechem, J. M., and E. Haas. 1989. Simultaneous determination of intramolecular distance distributions and conformational dynamics by global analysis of energy transfer measurements. *Biophys. J.* 55: 1225–1236.

Berlett, B. S., and E. R. Stadtman. 1997. Protein oxidation in aging, disease, and oxidative stress. *J. Biol. Chem.* 272:20313–20316.

Bevington, P. R. 1969. Data Reduction and Error Analysis for the Physical Sciences. McGraw-Hill, New York.

Blass, J. P. 1996. Cerebral metabolic impairments. *In* Alzheimer's Disease: Cause(s), Diagnosis, Treatment, and Care. Z. S. Khachaturian and T. S. Radebaugh, editors. CRC Press, Boca Raton, FL. 187–205

Blass, J. P., R. K.-F. Sheu, and G. E. Gibson. 2000. Inherent abnormalities in energy metabolism in Alzheimer disease. *Ann. N.Y. Acad. Sci.* 903: 204–221.

Browne, J. P., M. Strom, S. R. Martin, and P. M. Bayley. 1997. The role of beta-sheet interactions in domain stability, folding, and target recognition reactions of calmodulin. *Biochemistry.* 36:9550–9561.

Chapman, E. R., K. Alexander, T. Vorherr, E. Carafoli, and D. R. Storm. 1992. Fluorescence energy transfer analysis of calmodulin-peptide complexes. *Biochemistry.* 31:12819–12825.

Cheung, H. C. 1991. Resonance energy transfer. *In* Topics in Fluorescence Spectroscopy, Vol. 2. J. R. Lakowicz, editor. Plenum Press, New York. 128–176.

Chin, D., and A. R. Means. 1996. Methionine to glutamine substitutions in the C-terminal domain of calmodulin impair the activation of three protein kinases. *J. Biol. Chem.* 271:30465–30471.

Chin, D., and A. R. Means. 2000. Calmodulin: a prototypical calcium sensor. *Trends Cell Biol.* 10:322–328.

Chin, D., D. J. Soan, F. A. Quiocho, and A. R. Means. 1997a. Functional consequences of truncating amino acid side chains located at a calmodulin-peptide interface. *J. Biol. Chem.* 272:5510–5513.

Chin, D., K. E. Winkler, and A. R. Means. 1997b. Characterization of substrate phosphorylation and use of calmodulin mutants to address implications from the enzyme crystal structure of calmodulin-dependent protein kinase I. *J. Biol. Chem.* 272:31235–31240.

Crivici, A., and M. Ikura. 1995. Molecular and structural basis of target recognition by calmodulin. *Annu. Rev. Biophys. Biomol. Struct.* 24: 85–116.

Dado, G. P., and S. H. Gellman. 1993. Redox control of secondary structure in a designed peptide. *J. Am. Chem. Soc.* 115:12609–12610.

Driver, A. S., P. R. Kodavanti, and W. R. Mundy. 2000. Age-related changes in reactive oxygen species production in rat brain homogenates. *Neurotoxicol. Teratol.* 22:175–181.

Elshorst, B., M. Hennig, H. Försterling, A. Diener, M. Maurer, P. Schulte, H. Schwalbe, C. Griesinger, J. Krebs, H. Schmid, T. Vorherr, and E. Carafoli. 1999. NMR solution structure of a complex of calmodulin with a binding peptide of the Ca^{2+} pump. *Biochemistry.* 38:12320–12332.

Fairclough, R. H., and C. R. Cantor. 1978. The use of singlet-singlet energy transfer to study macromolecular assemblies. *Methods Enzymol.* 48: 347–379.

Falchetto, R., T. Vorherr, J. Brunner, and E. Carafoli. 1991. The plasma membrane Ca^{2+} pump contains a site that interacts with its calmodulin-binding domain. *J. Biol. Chem.* 266:2930–2936.

Ferrington, D. A., H. Sun, K. K. Murray, J. Costa, T. D. Williams, and T. C. Squier. 2001. Selective degradation of oxidized calmodulin by the 20S proteasome. *J. Biol. Chem.* 276:937–943.

Findlay, W. A., S. R. Martin, K. Bechingham, and P. M. Bayley. 1995. Recovery of native structure by calcium binding site mutants of calmodulin upon binding of sk-MLCK target peptides. *Biochemistry.* 34: 2087–2094.

Gao, J., D. H. Yin, Y. Yao, H. Sun, Z. Qin, Ch. Schöneich, T. D. Williams, and T. C. Squier. 1998a. Loss of conformational stability in calmodulin upon methionine oxidation. *Biophys. J.* 74:1115–1134.

Gao, J., D. Yin, Y. Yao, T. D. Williams, and T. C. Squier. 1998b. Progressive decline in the ability of calmodulin isolated from aged brain to activate the plasma membrane Ca-ATPase. *Biochemistry.* 37: 9536–9548.

George, S. E., Z. Su, D. Fan, S. Wang, and J. D. Johnson. 1996. The fourth EF-hand of calmodulin and its helix-loop-helix components: impact on calcium binding and enzyme activation. *Biochemistry.* 35:8307–8313.

Gibson, G. E., L. C. Park, H. Zhang, S. Sorbi, and N. Y. Calingasan. 1999. Oxidative stress and a key metabolic enzyme in Alzheimer brains, cultured cells, and an animal model of chronic oxidative deficits. *Ann. N.Y. Acad. Sci.* 893:79–94.

Goldberg, J., A. C. Nairn, and J. Kuriyan. 1996. Structural basis for the autoinhibition of calcium/calmodulin-dependent protein kinase I. *Cell.* 84:875–887.

Gornal, A., C. Bardawill, and M. David. 1949. Determination of serum proteins by means of the biuret reaction. *J. Biol. Chem.* 177:751–766.

Haas, E., E. Katchalski-Katzir, and I. Steinberg. 1978. Effect of the orientation of donor and acceptor on the probability of energy transfer involving electronic transitions of mixed polarization. *Biochemistry.* 17:5064–5070.

Haiech, J., M.-C. Kilhoffer, T. J. Lukas, T. A. Craig, D. M. Roberts, and D. M. Watterson. 1991. Restoration of the calcium binding activity of mutant calmodulins toward normal by the presence of a calmodulin binding structure. *J. Biol. Chem.* 266:3427–3431.

Hinds, T. R., and T. J. Andreasen. 1981. Photochemical cross-linking of azidocalmodulin to the (Ca^{2+}-Mg^{2+})-ATPase of the erythrocyte membrane. *J. Biol. Chem.* 256:7877–7882.

Hühmer, A. F. R., N. C. Gerber, P. R. Ortiz de Montellano, and C. Schöneich. 1996. Peroxynitrite reduction of calmodulin stimulation of neuronal nitric oxide synthase. *Chem. Res. Toxicol.* 9:484–491.

Ikura, M., G. M. Clore, A. M. Gronenborn, G. Zhu, C. B. Klee, and A. Bax. 1992. Solution structure of calmodulin-target peptide complex by multidimensional NMR. *Science.* 256:632–638.

James, P., M. Maeda, R. Fischer, A. K. Verma, J. Krebs, J. T. Penniston, and E. Carafoli. 1988. Identification and primary structure of a calmodulin binding domain of the Ca^{2+} pump of human erythrocytes. *J. Biol. Chem.* 263:2905–2910.

Jarrett, H. W., and J. Kyte. 1979. Human erythrocyte calmodulin: further chemical characterization and the site of its interaction with the membrane. *J. Biol. Chem.* 254:8237–8244.

Johnson, M. L., and L. M. Faunt. 1992. Parameter estimation by least-squares methods. *Methods Enzymol.* 210: 1–37.

Katz, A. M. 1992. Heart failure. *In* Physiology of the Heart. Raven Press, New York. 638–668.

Kondo, R., S. B. Tikunova, M. J. Cho, and J. D. Johnson. 1999. A point mutation in a plant calmodulin is responsible for its inhibition of nitric-oxide synthase. *J. Biol. Chem.* 274:36213–36218.

Kosk-Kosicka, D., and T. Bzdega. 1988. Activation of the erythrocyte Ca^{2+}-ATPase by either self-association or interaction with calmodulin. *J. Biol. Chem.* 263:18184–18189.

Lakowicz, J. R., H. Cherek, B. P. Maliwal, and E. Gratton. 1985. Time-resolved fluorescence anisotropies of diphenylhexatriene and perylene in solvents and lipid bilayers obtained from multifrequency phase-modulation fluorometry. *Biochemistry.* 24:376–383.

Lakowicz, J. R., and I. Gryczynski. 1991a. Frequency-domain fluorescence spectroscopy. *In* Topics in Fluorescence Spectroscopy, Vol. 1. J. R. Lakowicz, editor. Plenum Press, New York. 293–335.

Lakowicz, J. R., I. Gryczynski, W. Wiczk, J. Kúsba, and M. L. Johnson. 1991b. Correction for incomplete labeling in the measurement of distance distributions by frequency-domain fluorometry. *Anal. Biochem.* 195:243–254.

Lanzetta, P. A., L. J. Alvarez, P. S. Reinsch, and O. A. Candia. 1979. An improved assay for nanomole amounts of inorganic phosphate. *Anal. Biochem.* 100:95–97.

Levine, R. L., B. S. Berlett, J. Moskovitz, L. Mosoni, and E. R. Stadtman. 1999. Methionine residues may protect proteins from critical oxidative damage. *Mech. Ageing Dev.* 107:323–332.

Levine, R. L., L. Mosoni, B. S. Berlett, and E. R. Stadtman. 1996. Methionine residues as endogenous antioxidants in proteins. *Proc. Natl. Acad. Sci. U.S.A.* 93:15036–15040.

Meador, W. E., A. R. Means, and F. A. Quiocho. 1992. Target enzyme recognition by calmodulin: 2.4 Å structure of a calmodulin-peptide complex. *Science.* 257:1251–1255.

Meador, W. E., A. R. Means, and F. A. Quiocho. 1993. Modulation of calmodulin plasticity in molecular recognition on the basis of x-ray structure. *Science.* 262:1718–1721.

Meyer, D. F., Y. Mabuchi, and Z. Grabarek. 1996. The role of Phe^{92} in the Ca^{2+}-induced conformational transition in the C-terminal domain of calmodulin. *J. Biol. Chem.* 271:11284–11290.

Mukherjea, P., J. F. Maune, and K. Bechingham. 1996. Interlobe communication in multiple calcium-binding site mutants of *Drosophila* calmodulin. *Protein Sci.* 5:468–477.

Nelson, D. P., and L. A. Kiesow. 1972. Enthalpy of decomposition of hydrogen peroxide by catalase at 25°C with molar extinction coefficients of H_2O_2 in the UV. *Anal. Biochem.* 49:474–478.

Niggli, V., J. T. Penniston, and E. Carafoli. 1979. Purification of the (Ca^{2+}-Mg^{2+})-ATPase from human erythrocyte membranes using a calmodulin affinity column. *J. Biol. Chem.* 254:9955–9958.

O'Neil, K. T., and W. F. DeGrado. 1990. How calmodulin binds its targets: sequence independent recognition of amphiphilic alpha-helices. *Trends. Biochem. Sci.* 15:59–64.

Richardson, J. S., and D. C. Richardson. 1989. Principles and patterns of protein conformation. *In* Prediction of Protein Structure and the Principles of Protein Conformation. G. D. Fasman, editor. Plenum Press, New York. 1–98

Rose, G. D., A. R. Geselowitz, G. J. Lesser, R. H. Lee, and M. H. Zehfus. 1985. Hydrophobicity of amino-acid residues in globular proteins. *Science.* 229:834–838.

Sackett, D. L., and D. Kosk-Kosicka. 1996. The active species of plasma membrane Ca^{2+}-ATPase are a dimer and a monomer-calmodulin complex. *J. Biol. Chem.* 271:9987–9991.

Schenck, H. L., G. P. Dado, and S. H. Gellman. 1996. Redox-triggered secondary structure changes in the aggregated states of a designed methionine-rich peptide. *J. Am. Chem. Soc.* 118:12487–12494.

Sohal, R. S., and R. Weindruch. 1996. Oxidative stress, caloric restriction, and aging. *Science.* 273:59–63.

Squier, T. C., and D. J. Bigelow. 2000. Protein oxidation and age-dependent alterations in calcium homeostasis. *Frontiers Biosci.* 5:1–23.

Steiner, R. F., S. Albaugh, and M. C. Kilhoffer. 1991. Distribution of separations between groups in an engineered calmodulin. *J. Fluoresc.* 1:15–22.

Strasburg, G. M., M. Hogan, W. Birmachu, D. D. Thomas, and C. F. Louis. 1988. Site-specific derivatives of wheat germ calmodulin. *J. Biol. Chem.* 263:542–548.

Sun, H., J. Gao, D. A. Ferrington, H. Biesiada, T. D. Williams, and T. C. Squier. 1999. Repair of oxidized calmodulin by methionine sulfoxide reductase restores ability to activate the plasma membrane Ca-ATPase. *Biochemistry.* 38:102–112.

Sun, H., and T. C. Squier. 2000. Ordered and cooperative binding of opposing globular domains of calmodulin to the plasma membrane Ca-ATPase. *J. Biol. Chem.* 275:1731–1738.

Trewhella, J. 1992. The solution structures of calmodulin and its complexes with synthetic peptides based on target enzyme binding domains. *Cell Calcium.* 13:377–390.

Turrens, J. F. 1997. Superoxide production by the mitochondrial respiratory chain. *Biosci. Rep.* 17:3–8.

Verkhratsky, A., A. Shmigol, S. Kirischuk, N. Pronchuk, and P. Kostyuk. 1994. Age-dependent changes in calcium currents and calcium homeostasis in mammalian neurons. *Ann. N.Y. Acad. Sci.* 747:365–381.

Viner, R. I., D. A. Ferrington, T. D. Williams, D. J. Bigelow, and C. Schöneich. 1999. Protein modification during biological aging: selective tyrosine nitration of the SERCA2a isoform of the sarcoplasmic reticulum Ca^{2+}-ATPase in skeletal muscle. *Biochem. J.* 340:657–669.

Vogt, W. 1995. Oxidation of methionyl residues in proteins: tools, targets, and reversal. *Free Radic. Biol. Med.* 18:93–105.

Vorherr, T., P. James, J. Krebs, A. Enyedi, D. J. McCormick, J. T. Penniston, and E. Carafoli. 1990. Interaction of calmodulin with the calmodulin binding domain of the plasma membrane Ca^{2+} pump. *Biochemistry.* 29:355–365.

Vorherr, T., T. Kessler, F. Hofmann, and E. Carafoli. 1991. The calmodulin-binding domain mediates self-association of the plasma membrane Ca^{2+} pump. *J. Biol. Chem.* 266:22–27.

Weber, G. 1981. Resolution of the fluorescence lifetimes in a heterogeneous system by phase and modulation measurements. *J. Phys. Chem.* 85:949–953.

Williams, R. J. P. 1999. Calcium: the developing role of its chemistry in biological evolution. *In* Calcium as a Cellular Regulator. E. Carafoli and C. Klee, editors. Oxford University Press, Oxford. 3–54

Yan, L. J., R. L. Levine, and R. S. Sohal. 1997. Oxidative damage during aging targets mitochondrial aconitase. *Proc. Natl. Acad. Sci. U.S.A.* 94:11168–11172.

Yan, L. J., and R. S. Sohal. 1998. Mitochondrial adenine nucleotide translocase is modified oxidatively during aging. *Proc. Natl. Acad. Sci. U.S.A.* 95:12896–12901.

Yao, Y., C. Schöneich, and T. C. Squier. 1994. Resolution of structural changes associated with calcium activation of calmodulin using frequency domain fluorescence spectroscopy. *Biochemistry.* 33: 7797–7810.

Yao, Y., J. Gao, and T. C. Squier. 1996a. Dynamic structure of the calmodulin-binding domain of the plasma membrane Ca-ATPase in native erythrocyte ghost membranes. *Biochemistry.* 35:12015–12028.

Yao, Y., and T. C. Squier. 1996. Variable conformation and dynamics of calmodulin complexed with peptides derived from the autoinhibitory domains of target proteins. *Biochemistry.* 35:6815–6827.

Yao, Y., D. Yin, G. S. Jas, K. Kuczera, T. D. Williams, C. Schöneich, and T. C. Squier. 1996b. Oxidative modification of a carboxyl-terminal vicinal methionine in calmodulin by hydrogen peroxide inhibits calmodulin-dependent activation of the plasma membrane Ca-ATPase. *Biochemistry.* 35:2767–2787.

Yermolaieva, O., N. Brot, H. Weissbach, S. H. Heinemann, and T. Hoshi. 2000. Reactive oxygen species and nitric oxide mediate plasticity of neuronal calcium signaling. *Proc. Natl. Acad. Sci. U.S.A.* 97:448–453.

Yin, D., K. Kuczera, and T. C. Squier. 2000. Sensitivity of carboxyl-terminus methionines in calmodulin isoforms to oxidation by H_2O_2 modulates the ability to activate the plasma membrane Ca-ATPase. *Chem. Res. Toxicol.* 13:103–110.

Yin, D., H. Sun, R. F. Weaver, and T. C. Squier. 1999. Nonessential role for methionines in the productive association between calmodulin and the plasma membrane Ca-ATPase. *Biochemistry.* 38:13654–13660.